The Transition State for the Hydroxylation of Saturated Hydrocarbons with Hydroperoxonium Ion

Robert D. Bach* and Ming-Der Su

Contribution from the Department of Chemistry, Wayne State University, Detroit, Michigan 48202

*Received September 20, 1993. Revised Manuscript Received August 1, 1994**

Abstract: The 1,2-hydrogen shift in hydrogen peroxide (H_2O_2) to afford water oxide (H_2OO) has been studied at the QCISD, QCISD(T), and CASSCF levels of theory with a 6-31G* basis set. These data support the contention that the MP4SDTQ/6-31G*//MP2/6-31G* level provides adequate geometries and activation barriers for 1,2-hydrogen shifts in peroxides. The 1,2-hydrogen shift in protonated hydrogen peroxide ($H_3O_2^+$) has a barrier height of 32.5 kcal/mol at the MP4//MP2/6-31G** level. Activation barriers for the hydroxylation of methane, ethane, propane, butane, and isobutane at the MP4//MP2/6-31G* level of theory with perhydroxonium ion ($H_3O_2^+$) affording the corresponding protonated alcohols are predicted to be 5.26, 0.16, –4.64, –4.74, and –4.98 kcal/mol, respectively, when computed relative to isolated reactants. A reactent cluster between hydroperoxonium ion and isobutane is stabilized by 7.15 kcal/mol relative to isolated reactants, and the barrier height for insertion of HO^+ into isobutane is predicted to be 2.16 kcal/mol when computed from this gas phase reactant complex. This surprisingly low activation barrier is reduced to only 0.36 kcal/mol when zero-point energy corrections are included. The reaction trajectory for the approach of $H_3O_2^+$ to the hydrocarbon and the transition state structure is predicted on the basis of a frontier molecular orbital model that determines the orientation of attack of an electrophilic reagent E^+ on a doubly occupied canonical fragment molecular orbital of the hydrocarbon.

Introduction

Highly efficient selective oxidations of unactivated C–H bonds in saturated hydrocarbons typically come under the purview of biological processes.[1] However, recent oxygen insertion reactions involving highly reactive dioxiranes[2] and alkane hydroxylation with porphyrin P-450 models[3] have also been proven to be quite effective. Hydroxylation of hydrocarbons with oxygen donors such as trifluoroperoxyacetic acid[4a,b] and *p*-nitroperbenzoic acid[4c] provide alcohols by the formal insertion of HO^+ into the C–H σ bond. An oxygen insertion reaction into tertiary C–H bonds typically proceeds with retention of configuration. Relatively high regioselectivity is observed with the order of reactivity tertiary > secondary > primary C–H bonds. Electrophilic oxygenation of alkanes with ozone and hydrogen peroxide has also been studied by Olah and co-workers in superacid media.[5] The active electrophiles were assumed to be protonated ozone (HO_3^+) or hydroperoxonium ion ($HO–OH_2^+$). Hydroperoxonium ion was considered as the source of the incipient HO^+ ion that formed an intermediate pentacoordinate hydroxycarbonium ion transition state as illustrated below for the oxidation of isobutane (eq 1).[5a]

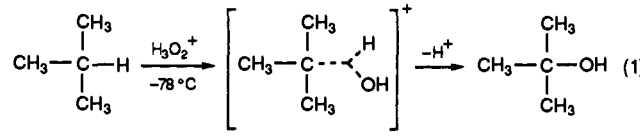

(1)

We have recently suggested a frontier molecular orbital (FMO) model for electrophilic oxygen atom insertion into saturated hydrocarbons.[6a] In this FMO model we dissect the nucleophilic hydrocarbon into doubly occupied fragment orbitals that have σ-like and π-like symmetry.[7] The requisite canonical Hartree–Fock (HF) molecular orbitals for the secondary carbon of propane are given in Scheme 1. For example, the π_{CH_2} fragment orbital shown has a mirror plane bisecting the two hydrogens shown and the molecular orbital containing the carbon 2p atomic orbital and two hydrogens has π-like symmetry. The two methyl groups are at 90° with respect to the plane of the CH_2 fragment and are included simply for purposes of visualization. In this qualitative theoretical treatment we identify the electrophile E as having an empty electrophilic orbital that can interact with a filled hydrocarbon fragment orbital that has one or more pairs of electrons that can serve as the terminus for a concerted 1,2-hydrogen migration. In the transition state electrophile E approaches the hydrocarbon fragment molecular orbital along the axis of its filled atomic carbon p orbital and a 1,2-hydrogen migration to the adjacent pair of electrons takes place in concert with C–E bond formation. We prefer to use a canonical MO

* Abstract published in *Advance ACS Abstracts*, September 15, 1994.

(1) (a) Cytochrome P-450: *Structure Mechanism and Biochemistry*; Ortiz de Montellano, P. R., Ed.; Plenum: New York, 1986. (b) Ortiz de Montellano, P. R. *Acc. Chem. Res.* **1987**, *20*, 289. (c) Hayano, M. In *Oxygenases*; Hayaishi, O., Ed.; Academic Press: New York, 1986; pp 181–240. (d) Ingold K. U. *Aldrichim. Acta* **1989**, *22*, 69.

(2) (a) Murray, R. W. *Chem. Rev.* **1989**, *89*, 1187. (b) Adam, W.; Curci, R.; Edwards, J. O. *Acc. Chem. Res.* **1989**, *22*, 205. (c) Murray, R. W.; Jeyareman, R.; Mohan, L. *J. Am. Chem. Soc.* **1986**, *108*, 2476. (d) Mello, R.; Rlorentlon, M.; Fusco, C.; Curci, R. *J. Am. Chem. Soc.* **1989**, *111*, 6749. (e) Adam, W.; Asensio, G.; Curci, R.; Gonzalez-Nunez, M. E.; Mello, R. *J. Org. Chem.* **1992**, *57*, 953. (f) Mello, R.; Cassidei, L.; Fiorentino, M.; Fusco, C.; Hümmer, W.; Jäger, V.; Curci, R. *J. Am. Chem. Soc.* **1991**, *113*, 2205.

(3) (a) Groves, J. T.; McClusky, G. A.; White, R. E.; Coon, M. *J. Biochem. Biophys. Res. Commun.* **1978**, *81*, 154. (b) Groves, J. T.; Nemo, Th.E.; Meyers, R. S. *J. Am. Chem. Soc.* **1979**, *101*, 1032.

(4) (a) Deno, N. C.; Jedziniak, E. J.; Messer, L. A.; Meyer, M. D.; Stroud, S. G.; Tomezsko, E. S. *Tetrahedron* **1977**, *33*, 2503. (b) Hart, H. *Acc. Chem. Res.* **1971**, *4*, 337. (c) Schneider, H.-J.; Müller, W. *J. Org. Chem.* **1985**, *50*, 4609.

(5) (a) Olah, G. A.; Farooq, O.; Prakash, G. K. S. In *Activation and Functionalization of Alkanes*; Hill, C. L., Ed.; John Wiley and Sons: New York; 1989; p 27. (b) Olah, G. A.; Parker, D. G.; Yoneda, N. *Angew. Chem., Int. Ed. Engl.* **1978**, *17*, 909. (c) Olah, G. A.; Yoneda, N.; Parker, D. G. *J. Am. Chem. Soc.* **1977**, *99*, 483. (d) Olah, G. A.; Yoneda, N.; Parker, D. G. *J. Am. Chem. Soc.* **1976**, *98*, 5261. (e) Olah, G. A.; Parker, D. G.; Yoneda, N.; Pelizza, F. *J. Am. Chem. Soc.* **1976**, *98*, 2245.

(6) (a) Bach, R. D.; Andrés, J. L.; Su, M.-D.; McDouall, J. J. W. *J. Am. Chem. Soc.* **1993**, *115*, 5768. (b) Bach, R. D.; Su, M.-D.; Aldabbagh, E.; Andrés, J. L.; Schlegel, H. B. *J. Am. Chem. Soc.* **1993**, *115*, 10237. (c) Bach, R. D.; Su, M.-D. Unpublished results. (d) Bach, R. D.; Owensby, A. L.; Gonzalez, C.; Schlegel, H. B.; McDouall, J. J. W. *J. Am. Chem. Soc.* **1991**, *113*, 6001. (e) Bach, R. D.; Andres, J. L.; Owensby, A. L.; Schlegel, H. B.; McDouall, J. J. W. *J. Am. Chem. Soc.* **1992**, *114*, 7207. (f) Bach, R. D.; Su, M.-D.; Andrés, J. L.; Schlegel, H. B. *J. Am. Chem. Soc.* **1993**, *115*, 8763.

(7) For a discussion see: Jorgensen, W. L.; Salem, L. *The Organic Chemist's Book of Orbitals*; Academic Press: New York, 1973.

0002-7863/94/1516-10103$04.50/0

Scheme 1. Hydrocarbon Fragment Orbitals for a Disubstituted Methylene Group That Can Interact with an Electrophile E

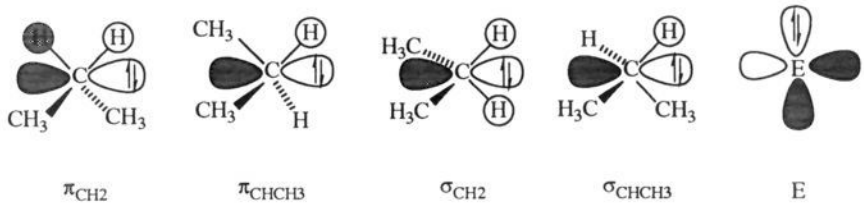

π_{CH2} π_{CHCH3} σ_{CH2} σ_{CHCH3} E

rather than the localized description of the C–H bond because it is easier to visualize the coalescence of the electron donor and acceptor if the approximate axis of the reaction can be more clearly defined.

To a first approximation the insertion product arises by the coalescence of atomic p orbitals of the fragment orbital and the electrophile E. The implication of a σ_{CH_2} or π_{CH_2} fragment orbital in propane identifies a molecular plane that is approached by E and provides an estimate of the starting geometry to search for a saddle point. However, a localized C–H orbital has essentially spherical symmetry and the electrophile can approach perpendicular to the C–H bond axis from any direction (i.e. 360°). The preferred donor–acceptor combination for insertion of water oxide (H_2O–O) into the σ C–H bond of a saturated hydrocarbon has been identified as a hydrocarbon fragment orbital with π-like symmetry (π_{CH_2}) and the electrophilic (empty) σ^* O–O orbital of water oxide.[6a] The transition state for this oxidation is shown in eq 2. The insertion of carbenes (CX_2 X = H, CH_3, F) into

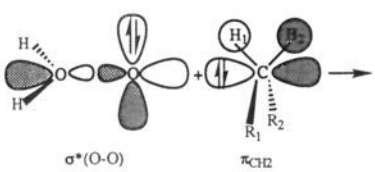

σ^*(O-O) π_{CH2}

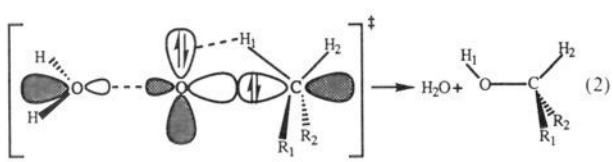

(2)

hydrocarbon C–H bonds proceeds by attack of a filled σ_{CH_2} *fragment orbital along the axis of the empty electrophilic atomic* p orbital of the carbene (CR_3R_4) with a concerted hydrogen migration to the carbene lone pair as shown in eq 3.[6b] Carbene

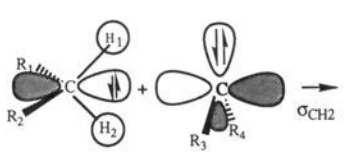

σ_{CH2}

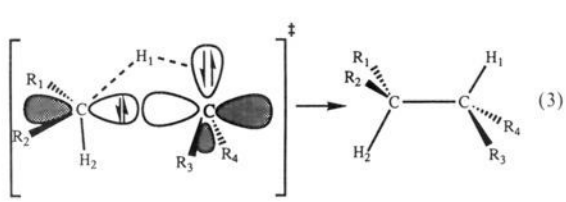

(3)

insertion in this σ_{CH_2} orientation has fewer steric interactions than a π_{CH_2} approach and provides the insertion product in its staggered lower energy conformation. The net molecular event involved in the insertion of singlet methylene ($^1CH_2$) into a C–H σ bond of methane is the formation of a new carbon–carbon σ bond. Consequently, this essentially barrierless reaction affords ethane with the attendant liberation of 104.0 kcal/mol (MP4//MP2/6-31G*). Despite the exothermicity of insertion reactions, a typical developing C–C bond distance in the TS is 2.13–2.15 Å. The insertion of singlet CH_2 into the oxygen–hydrogen bond of water[8] or methanol[6b] is also consistent with this FMO model. The insertion proceeds by interaction of an oxygen lone pair with the empty 2p orbital of the electrophilic carbene with a concerted hydrogen migration from oxygen to the lone pair of electrons on the adjacent carbon.

Since the π-like and σ-like canonical HF orbitals in hydrocarbons are typically very close in energy in the absence of perturbation by an electrophile, the orientation of the approach of the electrophile to the hydrocarbon fragment orbital will be largely determined by steric interactions. However, the axis of attack of the electrophile will be approximately aligned with an atomic 2p orbital of the carbon comprising the fragment orbital, and the σ and π nomenclature serves to identify the migrating hydrogen. This FMO model also allows one to predict the approximate reaction trajectory and transition state structure for the insertion of heavy metals (e.g. $ClRh(PH_3)_2$) into the C–H bonds of both alkanes and alkenes.[6c]

We now apply this theoretical model to the hydroxylation of saturated hydrocarbons with hydroperoxonium ion. Several peroxonium salts of $H_3O_2^+$ have been prepared and characterized.[9] Such oxygen transfer reagents exhibit an unusually high propensity to oxidize alkanes. We utilize the hydroperoxonium ion as the oxidant since it can formally transfer a hydroxyl cation (HO^+) to the hydrocarbon in concert with O–O bond rupture affording the neutral leaving group water. Conceptually, the mechanistic pathway outlined in eq 1 assumes attack of the electrophile at the C–H bond. We find, as predicted,[6a,b] that the electrophilic oxygen (HO^+) attacks the carbon atom and approaches the hydrocarbon along the approximate atomic 2p carbon orbital that comprises a σ_{CH_2} fragment orbital. This study also provides mechanistic insights for hydroxylation processes that can potentially serve to model biological oxygen insertion processes. Although hydrocarbon hydroxylation with cytochrome P-450 is generally thought to be a two-step process involving a free radical intermediate,[10a] more recent enzymatic oxidations of hydrocarbons to alcohols with methane monooxygenase are consistent with a concerted pathway for C–H bond insertion.[10b]

Method of Calculation

Molecular orbital calculations were carried out with the Gaussian 92 program system[11a] utilizing gradient geometry optimization.[11b] The geometries of the reactants and transition structures were first determined at the MP2/3-21G level of theory. All geometries were then fully optimized without geometry constraints using second-order Møller–Plesset perturbation theory (MP2/6-31G*). Relevant energies and barrier heights were computed with the 6-31G* basis set using fourth-order

(8) Walch, S. P. *J. Chem. Phys.* **1993**, *98*, 3163.

(9) Christe, K. O.; Wilson, W. W.; Curtis, E. C. *Inorg. Chem.* **1979**, *18*, 2578.

(10) (a) McMurry, T. J.; Groves, J. T. In *Cytochrome P-450: Structure, Mechanism and Biochemistry*; Ortiz de Montellano, P. R., Ed.; Plenum Press: New York and London 1986; p 1. (b) Liu, K. E.; Johnson, C. C.; Newcomb, M.; Lippard, S. J. *J. Am. Chem. Soc.* **1993**, *115*, 939.

(11) (a) Frisch, M. J.; Trucks, G. W.; Head-Gordon, M.; Gill, P. M. W.; Wong, M. W.; Foresman, J. B.; Johnson, B. G.; Schlegel, H. B.; Robb, M. A.; Replogle, E. S.; Gomperts, R.; Andres, J. L.; Raghavachari, K.; Binkley, J. S.; Gonzalez, C.; Martin, R. L.; Fox, D. J.; Defrees, D. J.; Baker, J.; Stewart, J. J. P.; Pople, J. A. GAUSSIAN 92; Gaussian, Inc.: Pittsburgh, PA, 1992. (b) Schlegel, H. B. *J. Comp. Chem.* **1982**, *3*, 214.

Table 1. Optimized Geometries and Energies for the 1,2-Hydrogen Shift in Hydrogen Peroxide[a]

	HF	MP2	MP4SDTQ[b]	QCISD	QCISD(T)	CCSD[c]	CASSCF[i]
			H_2O_2 (1)				
$R(O_1O_2)$, Å	1.397	1.468	1.482	1.465	1.480	1.442	1.495
$R(O_1H_1)$, Å	0.949	0.976	0.978	0.975	0.977	0.961	0.977
$\angle HO_1O_2$, deg	120.1	98.65	98.61	99.37	98.80	100.5	97.80
$\angle H_1O_1O_2H_2$, deg	115.4	121.0	121.0	119.3	120.9	111.2	121.3
			HOOH → H_2OO Transition State (TS-2)				
$R(O_1O_2)$, Å	1.602	1.576	1.633	1.656	1.661	1.614	1.660
$R(O_1H_1)$, Å	1.190	1.426	1.425	1.381	1.421	1.349	1.352
$R(O_2H_1)$, Å	1.094	1.035	1.038	1.052	1.044	1.038	1.063
$R(O_2H_2)$, Å	0.951	0.980	0.980	0.978	0.980	0.964	0.981
$\angle H_1O_1O_2$, deg	43.08	39.92	38.96	39.24	38.63	39.76	39.69
$\angle O_1O_2H_2$, deg	100.5	98.57	96.89	97.12	96.62	98.7	95.00
$\angle H_1O_1O_2H_2$, deg	106.0	104.1	104.2	104.2	104.1	103.8	103.0
			H_2OO (3)				
$R(O_1O_2)$, Å	1.606	1.517	1.563	1.573	1.578	1.534	1.596
$R(O_2H_1)$, Å	0.951	0.979	0.980	0.976	0.978	0.964	0.979
$\angle H_1O_2O_1$, deg	103.1	100.9	99.51	99.73	98.93		97.89
$\angle H_1O_2O_1H_2$, deg	112.1	109.4	108.5	103.2	102.4		106.2
$\Delta E_1^{\ddagger}$,[d] kcal/mol	57.6	58.0	53.4	52.5[e]	51.4[f]	52.4[g]	50.0[j]
$\Delta E_2^{\ddagger}$,[d] kcal/mol	18.0	4.7	3.7	4.2[e]	2.7[f]	3.2[h]	8.50[j]

[a] All calculations with the 6-31G* basis set, unless specified otherwise. [b] MP2 energies are full; MP4 energies are frozen core. [c] Data from C. Meredith, T. P. Hamilton, and H. F. Schaefer (*J. Phys. Chem.* **1992**, *96*, 9250), CCSD on TZ2p+f basis set. [d] HF, MP2, and MP4 barrier energies are with zero-point energies. [e] $\Delta E^{\ddagger}$ refers to QCISD/6-31G*//QCISD/6-31G* + zero-point energy at QCISD/6-1G*//QCISD/6-31G*. [f] $\Delta E^{\ddagger}$ refers to QCISD(T)/6-31G*//QCISD(T)/6-31G* + zero-point energy at QCISD/6-31G*//QCISD/6-31G*. [g] $\Delta E^{\ddagger}$ refers to CCSD(T)/TZ2P+f//CCSD/TZ2P+f. The zero-point energies are not included. [h] $\Delta E^{\ddagger}$ refers to CCSD(T)/TZ2P+f//CCSD/TZ2P+f + zero-point energy at CSD(T)/TZ2P+f//CISD/DZP. [i] CASSCF was calculated at 14-electron/10-orbital (14e/10orb). [j] $\Delta E^{\ddagger}$ refers to CASSCF(14e/10orb)//CASSCF(14e/10orb). The zero-point energies are not included.

Møller–Plesset perturbation theory (frozen core, MP4SDTQ/6-31G*//MP2/6-31G*). Vibrational frequency calculations at the MP2/6-31G* level were used to characterize all stationary points as either minima (zero imaginary frequencies), first-order transition states (a single imaginary frequency), or second-order saddle points, SOSP (two imaginary frequencies).

Results and Discussion

Because of the potential involvement of a 1,2-proton shift in the $H_3O_2^+$ fragment during the hydroxylation process, the energetic requirements of the 1,2-hydrogen shift in hydroperoxonium ion should be addressed. Historical difficulties attending the 1,2-hydrogen shift in hydrogen peroxide[12a] prompted us to first firmly establish the level of theory essential for obtaining adequate geometries and energetics for a 1,2-hydrogen shift in a peroxide. From a computational perspective one could place the $H_2O_2 \rightleftharpoons H_2OO$ equilibrium in the same category as the acetylene–vinylidene ($HC{\equiv}CH \rightleftharpoons :C{=}CH_2$) rearrangement.[13] It took considerable effort by the theoretical community to provide concincing data to support the intermediacy of vinylidene. The relatively high calculated barrier (~43 kcal/mol) for this acetylene rearrangement, which is comparable in magnitude to that for the H_2O_2 rearrangement, is now in excellent agreement with experiment.[13a] In earlier studies[6d,e] we have reported that the potential energy surface for the 1,2-hydrogen shift in hydrogen peroxide (eq 4) remains almost unchanged at the Hartree–Fock (HF) level over a broad range of basis sets up to and including the 6-311++G(2d,2p) basis. Calculations at the HF level with

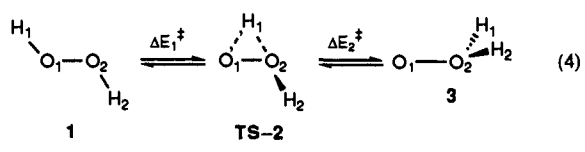

this relatively large basis set predict that H_2OO does not exist since the barrier ($\Delta E_2^{\ddagger}$) for reversion of water oxide (H_2OO) to hydrogen peroxide (H_2O_2) is still slightly negative. These data suggested that calculations to support the existence of water oxide (oxywater) as an energy minimum did not need a more flexible basis set, but rather geometry optimization at levels of theory that include electron correlation. One of the more frequently used methods for incorporating electron correlation is Møller–Plesset perturbation theory. When the 1,2-hydrogen shift was studied at the MP2/6-31G* level we found a radically different energy profile.[6d] The MP4SDTQ/6-31G* barrier, when the transition structure was optimized at the MP2/6-31G* level (MP4SDTQ/6-31G*//MP2/6-31G*), was 56.0 kcal/mol for the forward reaction ($\Delta E_1^{\ddagger}$). Significantly, at this level of theory water oxide does exist as a local minimum 3.9 kcal/mol (with zero point energy correction, Table 1) lower in energy than transition state **2** (**TS-2**). We have also computed this energy surface with geometry optimization at full fourth-order perturbation theory (that includes the triples) and found that the overalll potential energy surface at MP4SDTQ/6-31G* did not deviate significantly from the MP2 surface. Further examination of the data in Table 1 also shows that neither the geometries nor the energies were changed in any significant manner at the QCISD/6-31G* level *with or without the triples*. These data suggest that the dynamic electron correlation at the MP2 level is adequate for both the geometries and barriers in this relatively simple rearrangement. However, one may still question the reliability of the HF wave function as an adequate reference point for this transformation. We therefore examined the effects of static electron correlation correction with a full valence (omitting only the 1s orbital) complete active space SCF (CASSCF) calculation. In general we found good agreement with the MP2 predicted geometry with the exception of the O–O bond distance which tends to be slightly elongated with CAS optimization because of the absence of dynamic correlation. In a previous calculation involving insertion of water oxide into the σ C–H bond of ethane where O–O bond cleavage is involved, we observed the O–O bond to be 0.3 Å longer in the TS when the geometry was predicted by CAS relative to a QCISD calculation.[6a] Thus, it appears as though the geometry of the TS is better obtained with a higher-order wave function to which we add additional dynamical

(12) (a) Pople, J. A.; Raghavachari, K.; Frisch, M. J.; Binkley, J. S.; Schleyer, P. v. R. *J. Am. Chem. Soc.* **1983**, *105*, 6389. (b) Meredith, C.; Hamilton, T. P.; Schaeffer, H. F., III, *J. Phys. Chem.* **1992**, *96*, 9250.

(13) (a) Chen, Y.; Jones, D. M.; Kinsey, J. L.; Fleld, R. W. *J. Chem. Phys.* **1989**, *91*, 288. (b) Gallo, M. M.; Hamilton, T. P.; Schaefer, H. F. *J. Am. Chem. Soc.* **1990**, *112*, 8714.

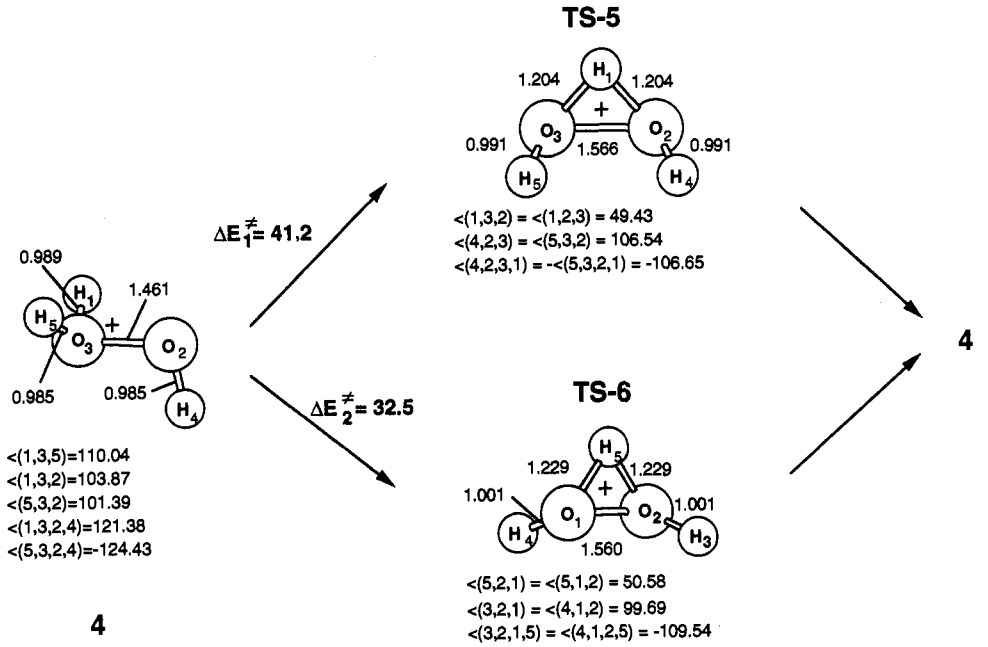

Figure 1. 1,2-Hydrogen shift in protonated hydrogen peroxide (**4**) at the MP2/6-31G** level of theory. The MP4//MP2/6-31G** energies for **4**, **TS-5**, and **TS-6** are −151.448 99, −151.383 36, and −151.363 19 au, respectively. Activation barriers are given in kcal/mol. The bond distances are given in Å and angles in deg.

correlation to obtain more reliable energies. Our conclusions[6d,e] concerning the existence of water oxide on the $H_2O_2 \rightleftharpoons H_2OO$ hypersurface have recently been verified by Schaefer et al.[12b] using couple cluster methods with single and double excitations (CCSD) with a triple-ξ plus double polarization (TZ 2p+f) basis set. These calculations predict a classical activation barrier for $H_2OO \rightarrow H_2O_2$ of 5.7 kcal/mol. After correction for zero-point vibrational energies the comparable ground state activation is 3.2 kcal/mol, in excellent agreement with our MP4 barrier of 3.6 kcal/mol (Table 1). This tetratomic species generated from a 1,2-hydrogen shift of a stable well-characterized structural isomer has a barrier for reversion to H_2O_2 that is slightly higher than that predicted for the vinylidene acetylene rearrangement.[13] This observation promoted the suggestion that water oxide may also be observed experimentally.[12b] The combined data given in Table 1 clearly indicate that a level of theory that includes electron correlation has a much greater impact upon the energetics of the $H_2O_2 \rightarrow H_2OO$ potential energy surface than inclusion of polarization functions in the basis set.

A 1,2-hydrogen shift to an adjacent electron lone pair in neutral molecules such as H_2O_2, NH_2OH, and HOF is predicted[12a,6d] to have a surprisingly high activation barrier ($\sim$50 kcal/mol). The magnitude of the energetic requirements for a comparable identity rearrangement in a protonated species such as hydroperoxonium ion **4** poses an intriguing question. A concerted 1,2-hydrogen shift in **4** may take place in both *cis* and *trans* conformations. Geometry optimization at the MP2/6-31G* level predicts that the activation energy ($\Delta E_2^{\ddagger}$ = 30.4 kcal/mol with ZPE) for rearrangement in cation **4** is 25.6 kcal/mol lower than that for a 1,2-hydrogen shift in neutral H_2O_2 (eq 4). The geometry of the transition state at the MP2/6-31G* level[6d] is not changed in any meaningful manner when polarization functions are added to the hydrogens. At the MP4/6-31G*//MP2/6-31G** level the predicted activation barriers for the 1,2-hydrogen shift identity reactions are predicted to be 32.5 and 41.2 kcal/mol.[14] The higher barrier for the *cis* conformation (**TS-5**) reflects the eclipsing of the adjacent hydrogens and lone pairs in the transition state (Figure 1). The above arguments concerning the 1,2-hydrogen shift in hydrogen peroxide (eq 4) support the reliability of the predicted magnitude of the activation barrier for the *cis*-**5** and *trans*-**6** transition states (MP4SDTQ/6-31G*//MP2/6-31G*) for the comparable 1,2-hydrogen shift in perhydroxonium ion **4**. Consequently, with barrier heights of this magnitude we can preclude the involvement of a concerted 1,2-hydrogen shift in ground state **4** and in the transition state for the hydroxylation of alkanes.

The hydroxylation of methane with $H_3O_2^+$ proceeds by the interaction of a π_{CH_2} fragment orbital (Scheme 1) with the σ^* O–O orbital in a manner quite analogous to that for oxygen insertion involving water oxide (eq 2). Although σ_{CH_2} orientation **8** (Figure 2) in the hydroxylation of methane has almost the identical energy as the π_{CH_2} approach in **TS-7**, the former is a second-order saddle point and the latter exhibits a single imaginary frequency. The net molecular event that takes place in this oxidation is the insertion of HO^+ into the σ_{C-H} bond, and the activation barrier for this process is 5.26 kcal/mol when measured from isolated reactants methane and perhydroxonium ion **4**. The O_1–H_3–C_2–H_5 dihedral angle of 180° in **TS-7** suggests an idealized π_{CH_2} approach of **4** to methane. Inclusion of polarization functions on the hydrogen atoms has only a modest effect on the transition structure geometry and its energetics. The bond distance of the transferring hydrogen (C_2–H_3) is 0.02 Å shorter while the O_1–H_3 bond distance slightly elongates with the 6-31G** basis set (Figure 2). The activation barrier for methane hydroxylation is reduced by 0.8 kcal/mol when a more flexible basis set is employed.

Both σ_{CH_2} and π_{CH_2} orientations were also examined for the oxidation of ethane. Electrophilic attack of **4** on ethane in the π_{CH_2} orientation as shown in **10** (Figure 2) afforded a stationary point with all forces below the convergence criteria that was only 0.37 kcal/mol higher in energy than isolated reactants (C_2H_6 and $H_3O_2^+$). The O_1–H_3–C_2–H_5 dihedral angle of 170° suggests that this approach deviates slightly from an idealized π_{CH_2} orientation (180° dihedral angle). An analytical frequency calculation showed that **10** was a SOSP that had two imaginary frequencies with the second one (53.3i cm^{-1}) corresponding to a rotation from the π_{CH_2} toward the σ_{CH_2} orientation. The actual first-order transition state for the hydroxylation of ethane, **TS-9**, has an approach of the O–O bond axis of the electrophilic perhydroxonium ion **4** that deviates significantly from an idealized (0° dihedral angle) σ_{CH_2} orientation ($\angle O_1$–H_3–C_2–H_5 = 27.0°).

(14) The MP2/6-31G** barriers for TS-5 and TS-6 are computed to be 40.9 and 31.9 kcal/mol and with zero point energy corrections these activation energies are 36.8 and 28.2 kcal/mol, respectively.

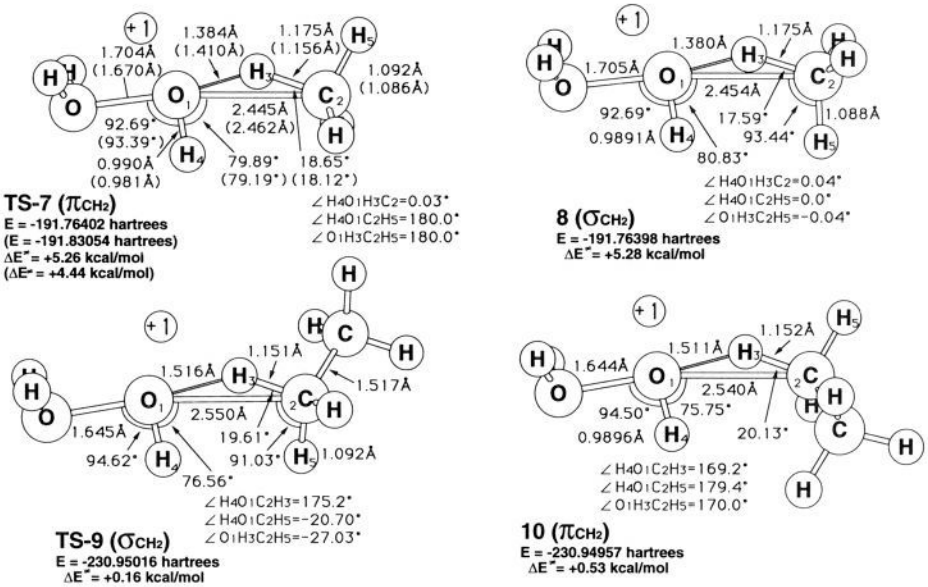

Figure 2. Transition states (**TS-7**, **TS-9**) and second order saddle points (**8**, **10**) showing the σ and π approaches for the hydroxylation of methane and ethane by hydroperoxonium ion. Geometries at MP2/6-31G* and total energies and activation barriers at MP4/6-31G*//MP2/6-31G* (MP-2/6-31G** geometry and MP4/6-31G**/MP2/6-31G** energies for **TS-7** are in parentheses). The MP4//MP2/6-31G* energies for **4**, CH_4, and C_2H_6 are –151.417 60, –40.354 79, –79.532 81 au, respectively. The MP4//MP2/6-31G** energies for **4** and CH_4 are –151.449 00 and –40.388 62 au, respectively.

The predicted barrier is essentially zero (0.16 kcal/mol) when measured from isolated reactants. However, the axis of attack defined by a filled σ_{CHR} orbital of the alkane and an empty O–O σ^* orbital of perhydroxonium ion **4** is in consonance with the FMO theory outlined above. In the TS, migration of hydrogen H_1 to the adjacent lone pair on oxygen occurs in concert with the O–O bond cleavage and the departure of the neutral leaving group water (eq 5). The kinetic product of this oxygen insertion

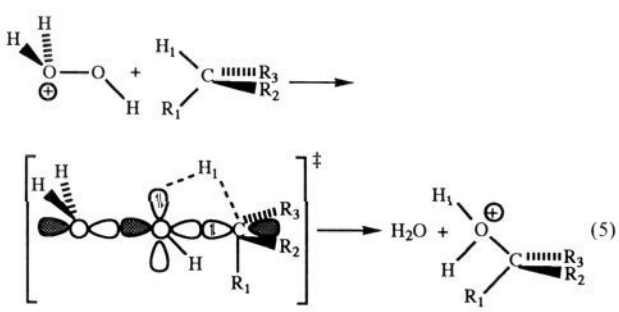

(5)

process is the corresponding protonated alcohol. The overall hydroxylation process involves both C–H and O–O bond breaking in concert with the formation of C–O and H–O σ bonds. The exothermicity of the formation of protonated ethanol from ethane is –79.07 kcal/mol.

The insertion of oxygen into the secondary σ_{C-H} bond of propane involves a highly symmetrical transition state (**TS-11**), and $H_3O_2^+$ approaches propane in a nearly idealized σ_{CH_2} manner ($\angle H_4$–O_1–C_2–H_5 = 0.17°). This is a facile oxidation reaction and the transition state (Figure 3) is below the energy of isolated reactants (–4.6 kcal/mol). The activation energy for the oxidation of butane at C_2 (**TS-12**) is essentially the same as that for propane; however, the lower symmetry in butane affords an unsymmetrical TS with significant deviation from the idealized σ_{CH_2} approach ($\angle O_1$–H_3–C_2–H_5 = 31.3°). The interaction of **4** with a filled hydrocarbon fragment orbital having σ-like symmetry does appear to be the preferred approach overall since the hydroxylation of isobutane (**TS-13**) proceeds in a σ_{CHCH_3} fashion despite the eclipsing of the O_1–H_4 bond with the C_2–C_5 σ bond ($\Delta E^\ddagger$ = –4.98 kcal/mol). Although computational restraints have precluded us from computing reactant complexes for all of the systems studied, we have located the gas-phase reactant cluster for perhydroxonium ion **4** and isobutane (**14**). This complex has a predicted O_1–C_2 bond distance of 3.326 Å (Figure 3) and lies 7.15 kcal/mol below isolated reactants. With a correction for basis set superposition error, the depth of this potential energy well is reduced by 0.69 kcal/mol. The molecular structure of complex **14** clearly reflects the orientation for approach of the reactants in **TS-13**. It is also evident that the electrophilic hydroxyl group is interacting with the carbon 2p orbital of a nearly idealized σ_{CHR} fragment orbital. The activation barrier for hydroxylation of isobutane is predicted to be 2.16 kcal/mol when computed from reactant cluster **14**, and this barrier is reduced to 0.36 kcal/mol when zero-point energies are included. Both **TS-11** and **TS-12** would also likely have small positive activation barriers if $\Delta E^\ddagger$ were computed from a reactant cluster.

The above gas-phase barriers for hydroxylation of hydrocarbons with perhydroxonium ion **4** suggest that this highly reactive oxidant does not appear to exhibit much discrimination for attack at secondary versus tertiary C–H bonds. The O_1–C_2 bond distance of 2.646 Å in **TS-13** suggests an early TS that has only a minor perturbation of the nucleophilic carbon atom. Hydroxylation with peroxy acids[4] appears to be more regioselective, but much higher temperatures are typically required for this less reactive oxidant. By comparison, water oxide is a high-energy isomer that lies 49.7 kcal/mol above ground state hydrogen peroxide,[6d,e] and its activation barriers (MP4/6-31G*//MP2/6-31G*) for oxidation of methane, ethane, propane, butane, and isobutane are predicted to be 10.7, 8.2, 3.9, 4.8, and 4.5, respectively, when computed relative to isolated reactants (H_2OO and hydrocarbon).[6a] The formation of methanol and water from water oxide and methane is a highly exothermic insertion reaction (–100.2 kcal/mol). The surprisingly low magnitude of activation barriers for $H_3O_2^+$ is consistent with experimental data. The electrophilicity of H_2O_2 can be markedly enhanced by addition of a strong acid to the level of one molar H^+ where rate increases of about two powers of ten have been observed.[15] The rate increases are due to specific acid catalysis involving a two-step process where the leaving group is neutral water. Hydroxylation of aromatic

(15) Edwards, J. O. In *Peroxide Reaction Mechanisms*; Edwards, J. O., Ed.; Interscience: New York, 1962; pp 67–106 and references therein.

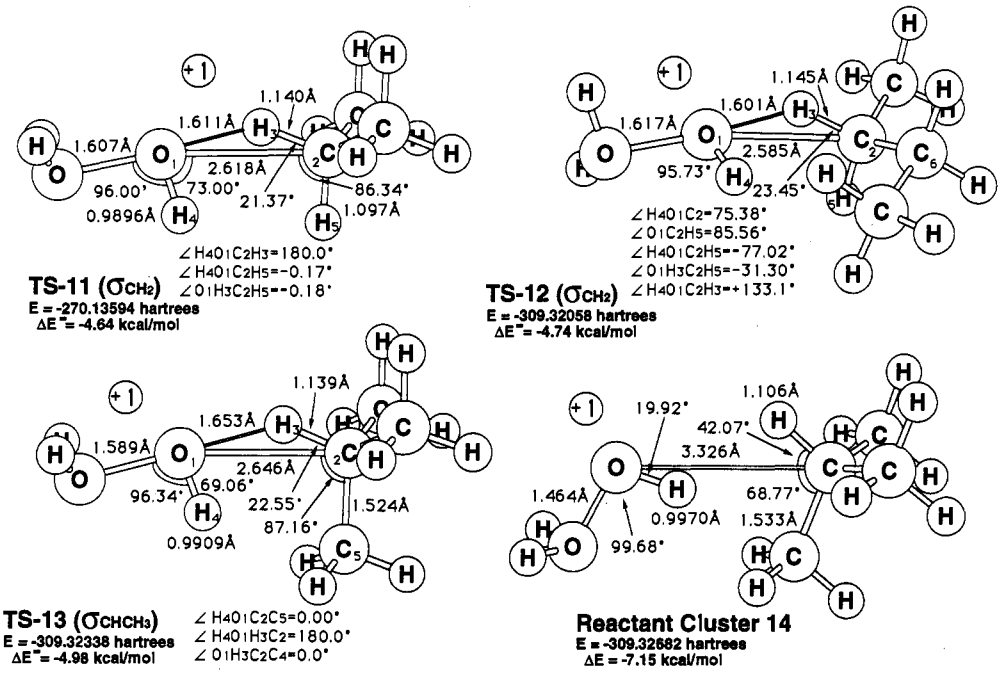

Figure 3. Transition state (**TS-11**, **TS-12**, **TS-13**) and reactant cluster (**14**) showing the σ approaches for the hydroxylation of propane, butane, and isobutane by hydroperoxonium ion. Geometries at MP2/6-31G* and total energies and activation barriers at MP4SDTQ/6-31G*//MP2/6-31G*. The MP4//MP2/6-31G* energies for propane, butane, and isobutane are −118.710 95, −157.895 42, and −157.897 84 au, respectively.

hydrocarbons[16a] and alkenes[16b] by H_2O_2 is only feasible in the

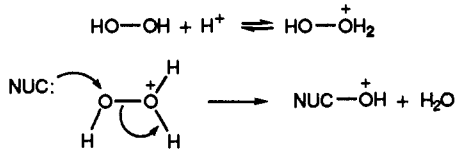

presence of strong acids. The electrophilic oxidation of saturated hydrocarbons is best achieved by the activation of H_2O_2 with magic acid (FSO_3H) in weakly nucleophilic solvents such as FSO_3H–SbF_5–SO_3 or FSO_3H–SbF_5–SO_2ClF.[5b] The fact that oxidation takes place readily at temperatures as low as −78 °C is consistent with the relatively low activation barriers that we have predicted computationally. Although hydroxylation reactions involving hydroperoxonium ions are often described as involving the hydroxyl cation derived from H_2O–OH^+, we hasten to point out that the calculated Mulliken charge on the electrophilic oxygen is −0.26 and that on the oxygen of the "water molecule" having a formal charge of +1 is −0.47. The net charge on the H_2O fragment in H_2O–OH^+ is +0.70.

The origin of the exalted electrophilicity of hydroperoxonium ion **4** can be traced in part to the relatively low energy of its LUMO. The computed (QCISD/6-31G*) LUMO's of H_2O_2, H_2OO, and $H_3O_2^+$ are 0.214, 0.161, and −0.118 au, respectively. The HOMO of $H_3O_2^+$ is also lower than one might anticipate since the HOMO's for these three oxidants are −0.477, −0.434, and −0.846 au, respectively. A HOMO–LUMO energy gap of 0.964 au is unusual and renders the frontier molecular orbitals of this reactive electrophilic species readily accessible to mix with the HOMO of the alkane. For example, the computed HOMO–LUMO orbital energies for isobutane are −0.4571 and +0.2219 au. The electrophilic properties of water oxide and perhydroxonium ion are consistent with the coordination of a water molecule to the ^1D state for the O atom and the $^1\Delta$ state for HO^+. However, the O–O bonds in both oxidants are relatively strong.

One of the basic tenets of this FMO theory is that insertion of an electrophilic reagent into a C–H bond involves the entire CH_2 fragment orbital and not just an isolated C–H σ bonding orbital. Examination of the single imaginary frequency for hydroxylation of methane (**TS-7**, Figure 4) provides excellent confirmation of this concept where E^+ attacks the π_{CH_2} fragment orbital along the axis of the carbon 2p orbital. The reaction vectors include O–O bond breaking with O_1 moving toward carbon and H_1 migrating to the incipient hydroxyl cation (O_1H). Animation of this imaginary frequency clearly shows *a rocking motion of the entire* π_{CH_2} *fragment* (H_1–C–H_2) as indicated by the vectors on both H_1 and H_2. There is virtually no motion of the orthogonal π_{CH_2} fragment comprising H_3–C–H_4. The vibrational motion for the hydroxylation of the tertiary center in isobutane (**TS-13**, Figure 4) involves transfer of the hydroxyl cation (HO^+) to the tertiary carbon in concert with O–O bond breaking and hydrogen transfer to the adjacent oxygen atom. Very little motion of the methyl groups is noted in the TS as a consequence of their greater reduced mass. The major molecular motions involved are those of the electrophilic hydroxyl group (O_1H^+) vibrating between the departing water molecule and carbon with a very discernible transfer of the hydrogen atom to oxygen. The *tert*-butyl moiety does rotate after the barrier is crossed since the inserting electrophile (HO^+) must eventually be on the C–H bond axis in the product. For the sake of comparison we provide a plot of the vectors of the imaginary frequency for the hydroxylation of isobutane with water oxide (**TS-15**). The overall reaction coordinate is quite similar to that observed in **TS-13**.

Perhaps the most striking difference between the molecular motions observed for singlet methylene insertion[6b] and hydroxylation (HO^+) is the relatively long C–O bond and small O_1–C_1–H_1 bond angle. In **TS-13** the former is 2.65 Å and the latter is only 22.6°. As the O_1–C_1–H_1 bond angle approaches linearity, the geometry of the hydroxylation transition state has many characteristics resembling those of a free radical hydrogen abstraction. It is not inconceivable to us that hydrocarbon hydroxylation by a protonated iron(III) hydroperoxide[6f] has many features in common with the transition structures described above.

In summary, we have described a series of transition structures for the formal insertion of HO^+ into the C–H bonds of hydrocarbons. The hydroxylation of hydrocarbons has been predicted to involve the interaction of the electrophilic empty σ^* orbital of the O–O bond in $H_3O_2^+$ with a filled hydrocarbon

(16) (a) Kurtz, M. E.; Johnson, G. J. *J. Org. Chem.* **1971**, *36*, 3184. (b) Zajacek, J. G. *J. Org. Chem.* **1973**, *38*, 1145.

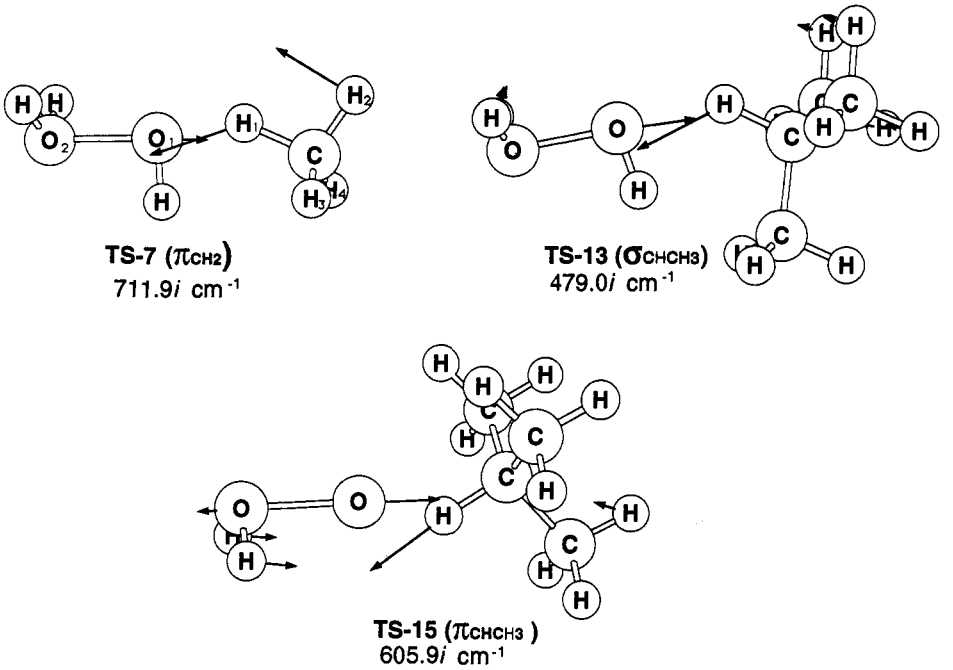

Figure 4. Reaction vectors for the single imaginary frequency describing the hydroxylation of methane (**TS-7**), the hydroxylation of isobutane (**TS-13**), and oxygen atom transfer from water oxide to isobutane (**TS-15**).

fragment orbital. With the exception of methane, hydrocarbons approach the axis of the O–O bond in an approximate σ_{CHR} orientation with attack of electrophilic oxygen at carbon. Hydrogen (H_3) migration occurs in concert with O–O bond rupture, and the O_1–C_2–H_3 bond angles in the transition structures vary from 19–24°. The C_2–H_3 bond distances for the migrating hydrogens vary from 1.175 Å for methane to 1.139 Å for insertion into isobutane. The carbon–electrophilic oxygen bond distances (C_2–O_1) exhibit the opposite trends and vary from 2.445 to 2.646 Å. Despite the established notion that saturated hydrocarbons are relatively unreactive, activation energies for this facile hydroxylation reaction are predictably low. The TS for hydroxylation with $H_3O_2^+$ comes earlier along the reaction coordinate than that for oxygen insertion with water oxide as evidenced by a longer C_2–O_1 bond distance (~0.3 Å). The transition structures described in this study are consistent with the overall FMO theory[6a–c] for insertion of electrophiles into the C–H bond of hydrocarbons. Extrapolation of these data to more complicated enzymatic hydroxylation processes is within the overall scope of this qualitative description of electrophilic attack at saturated σ bonds.

Acknowledgment. This work was supported in part by the National Science Foundation (CHE 93-06341) and a NATO Collaborative Research Grant (900707). We are also thankful to the Pittsburgh Supercomputing Center, CRAY Research, and the Ford Motor Company for generous amounts of computer time.